On the storm flow response of upland Alpine catchments

Stefano Orlandini,[1]* Andrea Perotti,[2] Giuseppe Sfondrini[2] and Alberto Bianchi[3]

[1]*Dipartimento di Ingegneria, Università degli Studi di Ferrara, Via Saragat 1, I-44100 Ferrara, Italy*
[2]*Dipartimento di Scienze della Terra, Università degli Studi di Milano, Via Mangiagalli 34,*
I-20133 Milano, Italy
[3]*Dipartimento di Ingegneria Idraulica, Ambientale e del Rilevamento, Politecnico di Milano,*
Piazza Leonardo da Vinci 32, I-20133 Milano, Italy

Abstract:

Detailed measurements of near-surface soil hydraulic conductivity, K_s, across the Bracciasco catchment (Central Italian Alps) are incorporated into a distributed, digital elevation model-based hydrological model to evaluate the effect of soil heterogeneity on catchment storm flow response. Surface and subsurface storm flow components are simulated for different distributions of K_s, including that obtained directly from measurements, that obtained by averaging measured data and others obtained on the basis of a simple functional parameter model. The reproduction of the catchment storm flow responses obtained using distributions of K_s based on measurements is satisfactory although an adjustment of such distributions is suggested to reproduce the hydrograph peaks owing to rapid surface runoff concentration and to improve the description of recession limbs at the same time. Numerical experiments indicate that the simulated storm flow response of the study catchment is substantially insensitive to near-surface soil heterogeneity in as far as the predominant mechanism of channel storm flow generation is subsurface flow. However, K_s is found to play an important role in the generation of overland flow during intense rainfall and, under these circumstances, monitoring of near-surface heterogeneity may be important to provide accurate descriptions of both surface and subsurface storm flow components. Copyright © 1999 John Wiley & Sons, Ltd.

KEY WORDS   upland alpine catchment storm flow; near-surface soil hydraulic conductivity; distributed modelling

INTRODUCTION

The spatial variability of the soil response to atmospheric forcing is of concern to engineers, geographers, hydrologists and soil scientists when simulating processes such as rainfall–runoff, erosion and sediment transport. At its present level of development, soil water physics provides quantitative infiltration theory and quantitative measurement techniques that enable useful quantitative predictions about the soil response to a given storm under certain circumstances. These circumstances are those of controlled experimentation on laboratory systems that are not too complicated and of simple field simulations. Difficulties arise when attempts are made to apply quantitative soil water physics over areas of any size in the field. It is hardly

* Correspondence to: Dr S. Orlandini, Dipartimento di Ingegneria, Universitá degli Studi di Ferrara, Via Saragat 1, I-44100 Ferrara, Italy. E-mail address: stefano@hydr.ing.unibo.it

surprising that known and unknown heterogeneities of many types, on many scales, can vitiate prediction based on theory developed for homogeneous soil water systems (Philip, 1980). The concept of spatial variability in hydrology must be viewed in terms of the scale under investigation. For a global water balance a single element may be the size of an entire continent or ocean. At the opposite end of the hydrological spectrum are detailed soil column experiments where soil grain size distributions are important (Loague and Gander, 1990). This work addresses evaluation of the effect of near-surface soil heterogeneity on surface and subsurface runoff delivery from steep, humid, forested mountain areas with very permeable soils, such as those normally encountered in upland Alpine catchments.

The rainfall–runoff process in upland Alpine areas can substantially be divided into three water transport phases describing: (1) flow into, through and out of saturated–unsaturated porous media; (2) hillslope rill flow; and (3) network channel flow. A model that rigorously couples these three water transport phases may be well suited as a research tool but is generally of little use as far as the operational hydrologist is concerned because of the staggering data requirements (Loague, 1990). In the model employed in the present study a certain degree of strictness in the coupling of catchment subprocesses is forfeited in exchange for simplicity and robustness in the flow dynamics description. This model is described in detail in Orlandini *et al.* (1996), Orlandini and Rosso (1996, 1998) and Orlandini (1997) and can be classed as a physically based-type model, as far as the model parameters reflect well-defined physical catchment features and thus they can be estimated from field measurements. The possibility of reproducing the storm flow response of a given catchment incorporating in a simplified model structure a reasonable set of field measurements is one of the main concerns of the present study.

DISTRIBUTED CATCHMENT MODELLING

On steep, humid, forested catchments with very permeable near-surface soils the discharge that is measured at the downstream end of a channel reach is likely to be supplied by channel inflow at the upstream end of the reach and by lateral inflows that enter the channel from the hillslope along the reach. These lateral inflows arrive at the channel in the form of groundwater, subsurface storm flow and/or overland flow. Groundwater provides a baseflow component to stream flow, while the flashy response in stream flow to individual precipitation events is usually ascribed to either subsurface storm flow or overland flow. Under intense rainfall events, where the surface soil layer becomes saturated to some depth, water is able to migrate through preferred pathways rapidly enough to deliver contributions to the stream during the peak runoff period (Mosley, 1979; Beven and Germann, 1982; Sloan and Moore, 1984).

In the present study the storm flow response of an upland Alpine catchment is reproduced by propagating local contributions to surface and subsurface runoff calculated at a set of non-interacting soil columns (described by digital elevation data and terrain attributes) throughout superficial and subsuperficial transport networks extracted from the catchment digital elevation model (DEM). The extraction of the superficial drainage network from DEM data is sketched in Figure 1 and the elemental system used to calculate local contributions to surface and subsurface runoff at each DEM cell is sketched in Figure 2. Detailed descriptions of the model components can be found in Orlandini *et al.* (1996) (soil response to storm events), Orlandini (1997) (soil response to atmospheric evaporative events) and Orlandini and Rosso (1996, 1998) (surface and subsurface flow routing). Attention is focused here on the model capabilities of reproducing the storm flow response of steep, humid, forested Alpine catchments with very permeable soils, with special emphasis to the role played by the near-surface soil heterogeneity. Under the circumstances encountered in such Alpine catchments, the two-layer soil columns of depth ($Z_{up} + Z_{low}$) at each elemental DEM cell (see Figure 2) can be assumed to constitute the soil profile above a relatively impervious bedrock and the g_{low} drainage flux can be viewed as the local contribution to subsurface storm flow.

At each elemental DEM cell of the discretized catchment the time compression approximation (TCA) soil water balance model developed in Orlandini *et al.* (1996) is used to calculate local contributions to
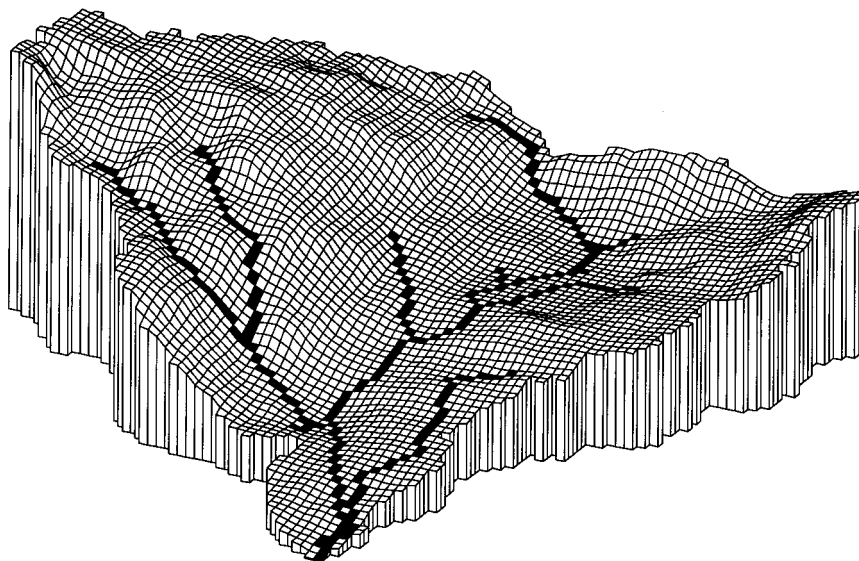
Figure 1. Bracciasco catchment DEM (50 m × 50 m resolution) showing the cells in which hillslope rill flow (white cells) and network channel flow (black cells) occur

infiltration excess surface runoff and subsurface storm flow runoff. This model is based on the Philip's (1954) two-parameter infiltration equation

$$f_{i*}(t) = \tfrac{1}{2}S_i t^{-1/2} + A_i \tag{1}$$

where f_{i*} is the infiltration capacity, t is time, S_i is the sorptivity and A_i is the gravitational infiltration rate. Equation (1) is an analytical solution to the partial differential equation that describes one-dimensional vertical infiltration [the Richards's (1931) equation] when water is ponded on a deep homogeneous soil with uniform initial water content. Parameters S_i and A_i have a physical significance and can be expressed incorporating the hydraulic properties of soil used in Brooks and Corey's (1964) constitutive equations (i.e. residual and saturated volumetric soil water contents, θ_r and θ_s, respectively; pore-size distribution index η; saturated soil matrix potential ψ_s; and saturated hydraulic conductivity K_s) and the initial degree of soil saturation

$$\Theta_i = \frac{Z_{up}}{Z_{up} + Z_{low}}\Theta_{up\,i} + \frac{Z_{low}}{Z_{up} + Z_{low}}\Theta_{low\,i}, \tag{2}$$

where $\Theta_{up\,i}$ and $\Theta_{low\,i}$ are the initial values for the average reduced soil moisture contents of the upper and lower control volumes, $\Theta_{up} = (\theta_{up} - \theta_r)/(\theta_s - \theta_r)$ and $\Theta_{low} = (\theta_{low} - \theta_r)/(\theta_s - \theta_r)$, respectively. Water yield from the elemental two-layer soil subsystem sketched in Figure 2 is calculated on the basis of the upper layer non-linear storage–outflow relationship

$$g_{up} = \max(f_i, K_s)\Theta_{up}^{(2+3\eta)/\eta} \tag{3}$$

where g_{up} is the soil control volume drainage and f_i is the actual infiltration rate, and of a similar relationship for the lower layer

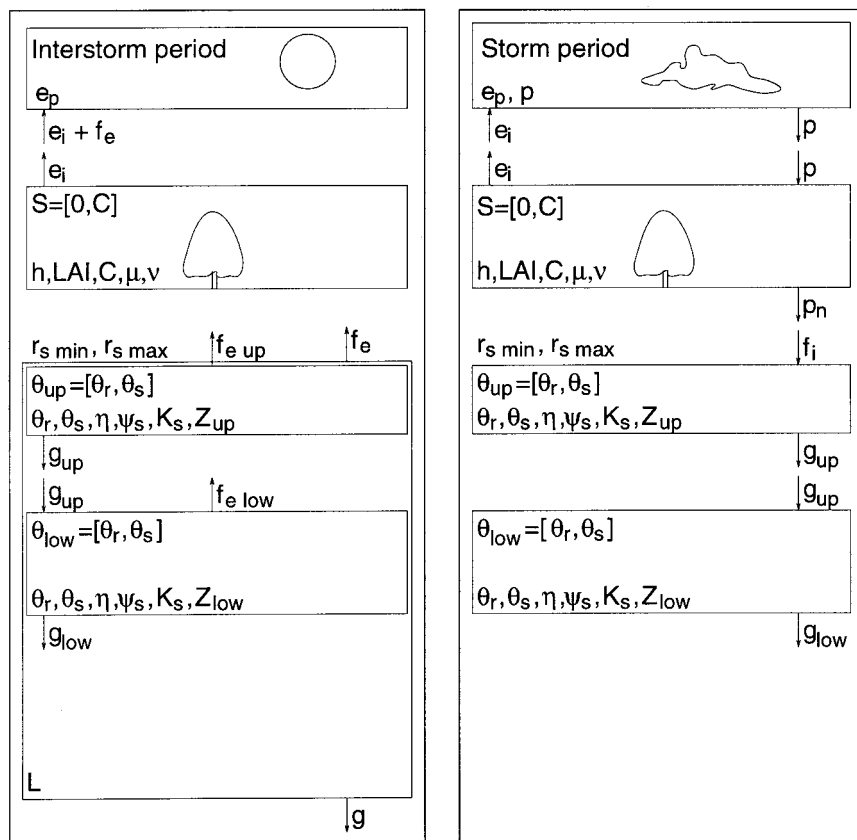$$g_{low} = \max(g_{up}, K_s)\Theta_{low}^{(2+3)\eta/\eta} \tag{4}$$

Figure 2. Conceptualization of the soil–vegetation–atmosphere continuum at the elemental catchment DEM cell. Notations are: S, canopy storage; C, canopy storage capacity; h, canopy height; *LAI*, leaf area index; μ and ν, coefficients of the canopy storage–outflow relationships; $r_{s\,min}$ and $r_{s\,max}$, minimum and maximum values of surface resistance to water vapour transfer, respectively; θ, volumetric water content; θ_r and θ_s, residual and saturated volumetric soil water contents; η, pore size distribution index; ψ_s, saturated soil matrix potential; K_s, saturated hydraulic conductivity; Z, soil layer depth; L, drying front depth; e_p, potential evaporation; p, gross precipitation; p_n, ground level precipitation; e_i, evaporation from the wet canopy; f_i and f_e, infiltration and exfiltration; g, drainage. Subscripts 'up' and 'low' indicate the upper and lower soil layer, respectively

(see Orlandini *et al.*, 1996). It is stressed here that the drainage flux from the lower soil layer, g_{low}, is assumed in this model application to constitute the local contribution to subsurface storm flow. The non-linear dependence of soil water yield g_{low} on the degrees of saturation, Θ_{up} and Θ_{low}, [Equations (3) and (4)] allows a modulated soil response during storming conditions. For high values of Θ_{up} and Θ_{low}, infiltrated water is rapidly released rather than accumulated in the control volumes, so as to describe the quick and intense contribution to subsurface storm flow caught by preferential paths in the soil domain. As Θ_{up} and Θ_{low} decrease, the ratios $g_{up}/\max(f_i, K_s)$ and $g_{low}/\max(g_{up}, K_s)$ decrease more than linearly and infiltrated water tends to be accumulated rather than released, so as to describe the slow release by saturated and unsaturated flow of the moisture that enters the soil matrix, which contributes to base flow discharge.

As equations (3) and (4) are highly non-linear with Θ_{up} and Θ_{low}, respectively, distributed estimates for initial conditions of soil saturation, $\Theta_{up\,i}$ and $\Theta_{low\,i}$, are particularly important and they are obtained here from discharge at the catchment outlet prior to storm rainfall, Q_i. Assuming that at the beginning of the simulation period: (1) this base flow discharge can be considered as being the overall delivery of uniformly distributed water yields from all the elemental DEM cell soil columns $g_{low\,i} = Q_i/A_{outlet}$, A_{outlet} being the

catchment area; (2) $\Theta_{\text{up}\,i} = \Theta_{\text{low}\,i} = \Theta_i$; and (3) $f_i \leqslant K_s$ (leading also to $g_{\text{up}} \leqslant K_s$), the initial status of soil saturation of each DEM cell can be calculated by inverting Equation (4) to obtain

$$\Theta_i = \min\left[\left(\frac{Q_i}{K_s A_{\text{outlet}}}\right)^{\eta/(2+3\eta)}, 1\right] \tag{5}$$

where the cut-off value 1 is introduced to avoid values of Θ_i greater than 1 for cells in which $K_s < Q_i/A_{\text{outlet}}$.

The idea of using initial discharge to estimate distributed catchment storage goes back to the TOPMODEL formulation developed in Beven and Kirkby (1979) and to the formulation developed in Troch *et al.* (1993a) on the basis of the Boussinesq's (1904) hydraulic groundwater equation. These works were successively extended by Sivapalan *et al.* (1987) and by Troch *et al.* (1993b), respectively, to provide soil moisture profiles from estimates of effective depth to the water table. The technique developed here can be viewed as a further extension of those developed in Beven and Kirkby (1979), Sivapalan *et al.* (1987) and Troch *et al.* (1993a,b), useful for applications to upland Alpine catchments, where the water table surface normally plays a different role with respect to lowland gently sloping catchments and where water yield from hillslopes is delivered to the catchment outlet in relatively short times.

Superficial and subsuperficial drainage networks are extracted automatically from the catchment DEM (see Orlandini and Rosso, 1996, 1998). Distinction between hillslope rill and network channel cells is based on the 'constant critical support area concept', as described in Montgomery and Foufoula-Georgiou (1993). Rill flow is assumed to occur for all those catchment cells for which the upstream drainage area A does not exceed the constant threshold value A_*, while channel flow is assumed to occur for all those cells for which A equals or exceeds A_*. The model routes storm flow runoff downstream from the uppermost DEM cell in the basin to the outlet, following the DEM-based drainage networks mentioned above. A given cell will receive water from its upslope neighbours and discharge to its downslope neighbours. For cells of flow convergence the upstream inflow hydrograph is taken as the sum of the outflow hydrographs of the neighbouring upslope cells from which the cell receives water. The catchment storm flow response is obtained as the sum of the surface and subsurface components. More precisely, infiltration excess runoff is propagated through the rill network over hillslopes until the network is reached and through the channel network towards the outlet, successively. Soil water released by the elemental soil columns that constitute the unsaturated hillslope is routed through the subsuperficial transport network until the channel is reached and is then converted to surface water and propagated via the channel network towards the outlet. At the present stage of model development, surface and subsurface yields from hillslopes are routed in the channel network separately, as the two flow components were linearly linked. Surface and subsurface water yield from hillslopes can be easily linked into a single lateral inflow term at the hillslope bases and propagated through the channel network, but this is not carried out here to allow evaluation of the different components to storm flow response at the catchment outlet.

The Muskingum–Cunge method with variable parameters developed by Ponce and Yevjevich (1978) on the basis of the diffusion wave formulation given by Cunge (1969) is used to describe hillslope rill flow, kinematic subsurface storm flow and network channel flow. Kinematic wave celerity, c_k, and hydraulic diffusivity, D_h, in the underlying convection–diffusion flow equation

$$\frac{\partial Q}{\partial t} + c_k \frac{\partial Q}{\partial s} = D_h \frac{\partial^2 Q}{\partial s^2} + c_k q_L \tag{6}$$

where s and t are the spatial and temporal coordinates, respectively, Q is the flow discharge and q_L is the lateral inflow, are calculated dynamically at each grid point of the discretized space–time domain and, as discussed in details by Ponce (1986), this allows the control of numerical diffusivity and leads to consistency and unconditional stability of the scheme. Surface and subsurface lateral inflows are obtained from local contributions to infiltration excess runoff and to subsurface storm flow runoff calculated at the

elemental cell systems sketched in Figure 2, and expressions of c_k and D_h obtained on the basis of the Manning–Gauckler–Strickler and Darcy friction equations are used in the surface and subsurface propagation processes, respectively (see Orlandini and Rosso, 1996, 1998). In particular, celerity $c_k^{(sub)}$ and diffusivity $D_h^{(sub)}$ of subsurface storm flows, which may occur in phreatic/perched aquifers with a bottom slope approximately equal to $S_0 = \sin \beta$, β being the land surface inclination angle, are expressed on the basis of the Darcy type flow equation

$$Q^{(sub)} = \Omega^{(sub)} K_h S_f \tag{7}$$

where $Q^{(sub)}$ is the subsurface storm flow discharge, $\Omega^{(sub)}$ is the apparent subsurface flow area (i.e. occupied by both solid particles and voids), K_h is the hydraulic conductivity of the subsuperficial path and S_f is the friction slope, yielding

$$c_k^{(sub)} = K_h S_0 \tag{8}$$

and

$$D_h^{(sub)} = \frac{Q^{(sub)} \cos \beta}{W^{(sub)} S_0} \tag{9}$$

$W^{(sub)}$ being the subsurface flow width (see Appendix). As the scheme of apparent porous medium is employed in the proposed formulation, $c_k^{(sub)}$ and $D_h^{(sub)}$ do not depend on soil porosity θ_s. This is consistent with the assumption that subsurface storm flows occur mainly in preferential paths of the soil domain rather than in a homogeneous soil matrix domain of porosity θ_s. It is also noted here that the expressions obtained for $c_k^{(sub)}$ and $D_h^{(sub)}$ allow the simulation of subsurface flow for variable hydrological/geomorphological conditions, ranging from convection-dominated to diffusion-dominated flows. Combination of this model capability with the non-linear description of soil water yield expressed by Equations (3) and (4) may therefore provide an efficient tool for describing both quick subsurface storm flow from steeply sloping hillslopes and delayed subsurface flow from lower slope areas, which contributes to baseflow (Mosley, 1979).

CATCHMENT APPLICATION

The model described in the previous section was applied to the Bracciasco catchment, located in the Central Italian Alps, near the city of Sondrio. The area of the Bracciasco catchment is $A_{outlet} = 9 \cdot 16$ km^2. The terrain is forested and mountainous, with an average elevation of 2133 m above sea level and an average land slope of about 38%. The elevation of the highest peak is 2900 m, and the outlet is at 1400 m above sea level. Geological, pedological and vegetational catchment features were surveyed and synthesized in a set of thematic maps by Bacchi *et al.* (1983). In the lower catchment areas a soil layer covers a relatively impervious glacial bedrock. With increasing elevation the soil layer depth decreases, leaving the bedrock formation exposed to physical and chemical atmospheric agents in the upper catchment areas. The hydraulic behaviour of the exposed fractured rock formations was found to be similar to that of the underlying coarse-grained deposits, allowing a certain continuity in the hydraulic description of the catchment land surface (Sfondrini, 1986). The terrain is forested in the lower part and covered by grass in the upper part, with vegetation height gradually decreasing with elevation. The climate is continental. The rainy season lasts from May until October, with peaks in June, July and August. The stream flow generation mechanism is mostly subsurface storm flow (especially from coarse-grained terrains and exposed fractured rocks in upland areas), but infiltration excess rainfall may also occur (especially from fine-grained lowland terrains) in response to rainfall peaks during intense storm conditions.
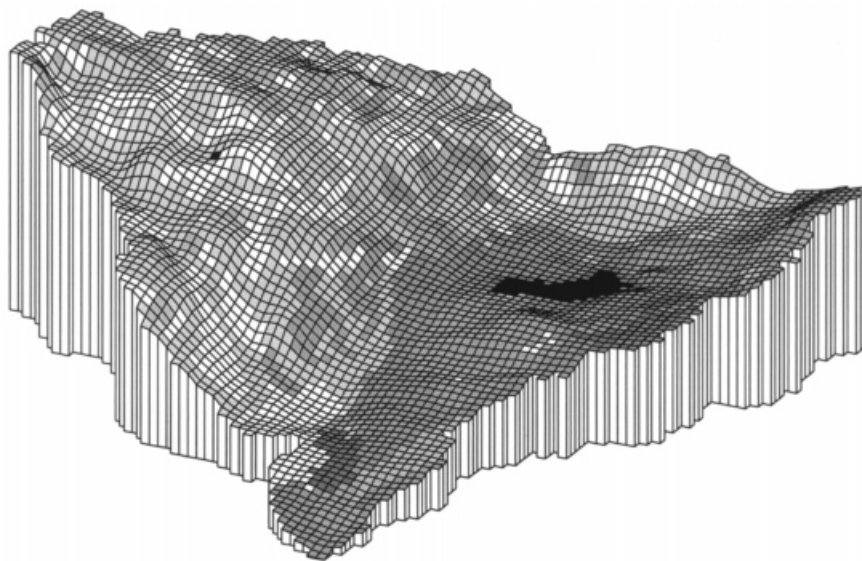
Figure 3. Bracciasco catchment DTM (50 m × 50 m resolution) showing the near-surface soil log-conductivity opposites ($pK_s = -\log_{10} K_s$), as obtained from field investigations, with the darker shades representing lower conductivities

The catchment area is horizontally discretized into 3665 cells with a 50-m grid spacing (Figure 1). The DEM is processed to obtain estimated distributed terrain slopes and automatically generated drainage networks, as mentioned in the previous section. Hillslope rill and network channel cells are identified through the 'critical support area concept' with constant threshold $A_* = 0.32$ km^2, corresponding to 128 DEM cells. This threshold area produces a network that compares very favourably with blue lines depicted in topographic maps at the scale 1 : 10 000 (Bacchi *et al.*, 1983). There is a small lake within the catchment (the Palù Lake) which has been treated in the digital catchment modelling as an impervious surface (black cells in Figure 3). The storage–outflow effects of the lake on catchment dynamics have not been explicitly described in the present work. Surface cover and soil hydraulic properties summarized in the sketch of Figure 2 are assigned to each DEM cell. An extensive field campaign has been carried out by the Dipartimento di Scienze della Terra of the Università degli Studi di Milano to provide a detailed survey of near-surface soil hydraulic conductivity, K_s, across the Bracciasco catchment (Chiari, 1984). The measurements collected have been combined with pedological and geological surveys to provide the classification summarized in Table I and the digital terrain model (DTM) shown in Figure 3. The infiltration experiments were made using single-ring infiltrometers. Infiltration rates were measured at frequent intervals throughout each experiment to develop complete infiltration curves. The durations of the infiltration experiments were

Table I. Classification of near-surface soil saturated hydraulic conductivity in the Bracciasco catchment

Class	Soil description	K_s (m s^{-1})	pK_s^*
1	Gravel, sand and silt/exposed fractured rocks	$5 \cdot 50 \times 10^{-2}$	1·26
2	Gravel, silt, and slightly clayish sand	$4 \cdot 50 \times 10^{-3}$	2·35
3	Gravelly sand and silt	$5 \cdot 50 \times 10^{-4}$	3·26
4	Gravelly sand and slightly clayish silt	$7 \cdot 50 \times 10^{-5}$	4·12
5	Sand and silt	$3 \cdot 00 \times 10^{-5}$	4·52
6	Sandy silt	$7 \cdot 50 \times 10^{-6}$	5·12
7	Clayish silt slightly sandy	$3 \cdot 00 \times 10^{-6}$	5·52
8	Clayish silt	$1 \cdot 00 \times 10^{-8}$	8·00

* Saturated hydraulic log-conductivity opposites, $pK_s = -\log_{10} K_s$.

constrained by the availability of water which had to be transported uphill across the steeply sloping Bracciasco catchment. At each location infiltration experiments were repeated until the difference between two consecutive measurements was adequately small. The final infiltration rate measured was assumed to be the near-surface soil saturated hydraulic conductivity, K_s.

Spatial distributions of all the other model parameters are expressed as exponential functions of the grid-cell elevations, where the values of the top and outlet cell parameters are considered to characterize these distributions. The exponential relationship is

$$p = p_{\text{outlet}} \exp\left[\frac{\ln(p_{\text{top}}/p_{\text{outlet}})}{z_{\text{top}} - z_{\text{outlet}}}(z - z_{\text{outlet}})\right] \tag{10}$$

where p, p_{outlet} and p_{top} represent the parameter values for an arbitrary cell, the outlet cell and the top cell, respectively, and z, z_{outlet} and z_{top} represent the corresponding cell elevations. As previously mentioned, for the Bracciasco catchment z_{outlet} and z_{top} equal 1400 and 2900 m a.s.l., respectively. The outlet and top cell values for all the model parameters are reported in Table II and represent reasonable values for the considered catchment area. Undoubtedly, there is substantial uncertainty for many of the parameter values used here (e.g. lower soil control volume depth, Z_{low}, Gauckler–Strickler roughness coefficient, k_S, for overland and channel flows and subsuperficial network conductivity, K_h) even though they were each selected carefully. In particular, soil column depth Z_{low} (see Figure 2) is found to be a critical model parameter for describing the variability of soil storage across the catchment. High values of Z_{low} are assigned to upland areas to reproduce the storage effects of deep fractured rock. Although these complex formations can hardly be surveyed, it appears realistic to assume great storage capacities for them on the basis of the observed discharges after storm cessation from many springs across the catchment. The Gauckler–Strickler roughness, k_S, of hillslope rills and network channels has been estimated on the basis of values published in

Table II. Characteristic values of the functional parameter model of Equation (10) used in the Bracciasco catchment application

Parameter	Outlet value	Top cell value
Soil–vegetation–atmosphere system (see Figure 2)		
h (m)	3·00	0·30
LAI	1·0	1·0
C (m)	$3·0 \times 10^{-3}$	$1·0 \times 10^{-3}$
μ	0·15	0·15
ν	3·00	3·00
$r_{s\,\text{min}}$ (m^{-1} s)	30	30
$r_{s\,\text{max}}$ (m^{-1} s)	700	700
θ_r	0·04	0·04
θ_s	0·70	0·50
η	0·20	0·60
ψ_s (m)	−0·15	−0·10
K_s (m s^{-1})	$3·06 \times 10^{-5}$	$1·68 \times 10^{-2}$
Z_{up} (m)	0·10	0·10
Z_{low} (m)	1·40	2·60
Superficial and subsuperficial hillslope networks		
k_S (m$^{1/3}$ s^{-1})	0·70	0·70
K_h^* (m s^{-1})	0·05†	0·05†
Superficial channel network		
k_S (m$^{1/3}$ s^{-1})	5·00	5·00

*Fitting parameter.
†Value in the range of those published by Mosley (1979).

the literature by Emmett (1978) and Bathurst (1993), respectively, while the subsuperficial network conductivity, $K_h = 0.05$ m s^{-1}, reported in Table II has been obtained by treating K_h as a fitting parameter. This value is in the range of those published by Mosley (1979) on the basis of dye-tracer experiments, which demonstrated that water may move through macropores at rates two order of magnitude greater than the saturated hydraulic conductivity of the soil matrix. Hence the hydraulic conductivity, K_h, used to characterize the subsurface storm flow must be regarded as different from that measured from small soil cores and, for catchment application of the model, it may be considered as an 'effective' parameter of the soil profile rather than being derived from the measured values of hydraulic conductivity for the soil matrix (Moore and Grayson, 1991).

In the application reported here, the effect of near-surface soil heterogeneity on the Bracciasco catchment storm flow response is investigated by varying only the distribution across the watershed of near-surface soil conductivity, K_s, which is recognized to be a critical parameter in infiltration and runoff simulations (e.g. Paniconi and Wood, 1993; Troch et al., 1993b). The values of K_s assigned to each catchment DTM cell on the basis of field measurements are plotted against cell elevation in Figure 4 and the data points obtained are interpreted by the functional parameter model of Equation (10). Four test cases are considered: (a) distribution of K_s obtained from field measurements, as represented in Figure 3 and Table I; (b) uniform distribution of K_s, with average measured value of 5.41×10^{-4} m s^{-1}; (c) functional distribution of K_s based on the model of Equation (10), with characteristic outlet and top cell values, 3.06×10^{-5} and 1.68×10^{-2} m s^{-1}, respectively, corresponding to the least-square interpretation of measurements; and (d) functional distribution of K_s based on the model of Equation (10), with adjusted outlet value
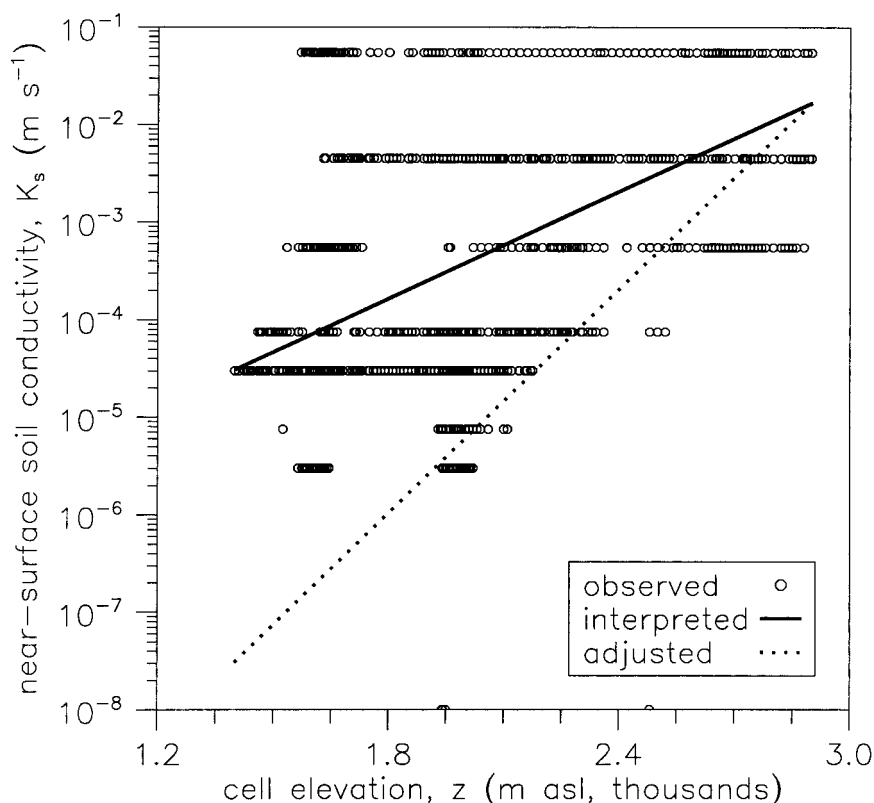

Figure 4. Distributions of near-surface soil conductivity in the Bracciasco catchment with cell elevation, as obtained from field measurements and from the functional parameter model of Equation (10)
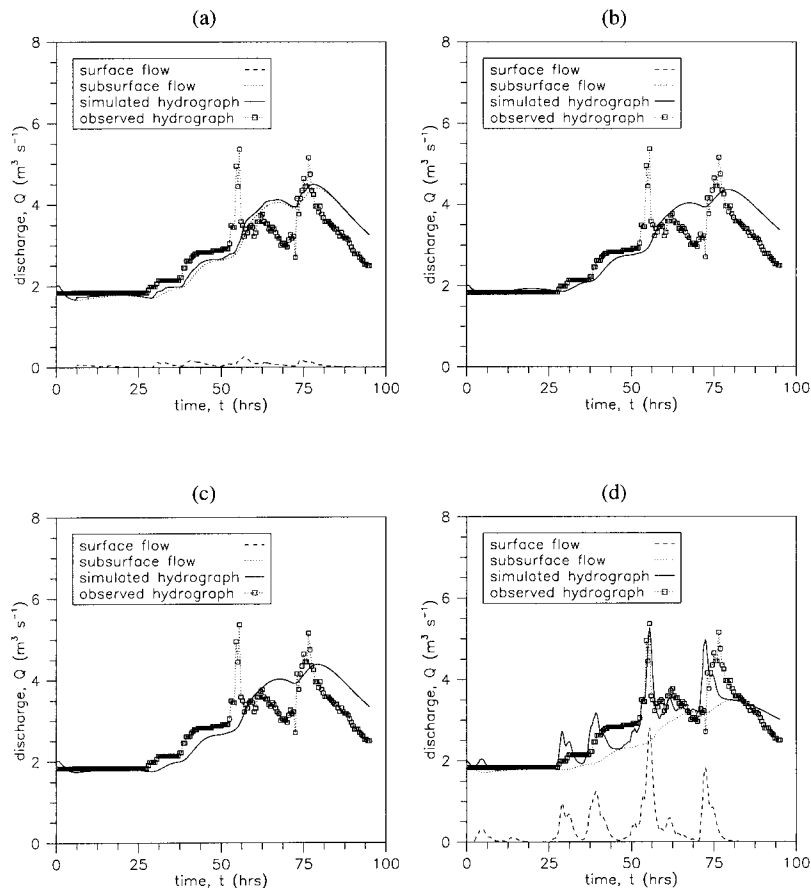
Figure 5. Simulated and observed Bracciasco catchment storm flow hydrographs during the 27 August–1 September 1977 flood event, for different distributions of near-surface soil conductivity: (a) measured K_s; (b) average measured K_s; (c) functional parameter model (10)-based K_s, adjusted. Surface and subsurface flow hydrographs are composed of infiltration excess and subsurface water yields from hillslopes, respectively

3.06×10^{-8} m s^{-1}, as justified later (Figure 4). The TCA water balance model developed in Orlandini *et al.* (1996) was run to calculate local contribution to infiltration excess surface runoff and subsurface storm flow runoff in response to storm events at 0·5-hour time-step resolution and the effect of soil heterogeneity on catchment storm flow response was investigated by comparing the simulation hydrographs corresponding to the above four test cases, (a)–(d). The results are shown in Figure 5 with reference to the flood event of 27 August–1 September 1977.

As shown in Figure 5a, incorporation of the near-surface soil conductivities obtained directly from field inspections [test case (a)] in the model structure produces a satisfactory reproduction of the overall catchment storm flow response. The simulation hydrographs confirm the supposed catchment attitude to deliver a dominant subsurface storm flow response with respect to the rainfall excess component. However, assuming (on the basis of simple visual analysis of the observed hydrograph shape) that the observed hydrograph peaks are a result of rapid surface runoff concentration during the periods of peak rainfall intensity, the simulated storm flow response appears to display an underestimated surface flow component during these peak rainfall periods and an overestimated subsurface flow component in the recession limbs soon afterwards. This may suggest that the simulated partitioning of ground-level precipitation at the land surface

obtained from the explicit incorporation of measured soil conductivities should be adjusted to produce better simulation results. In addition, it is relevant to note that the procedure introduced in the previous section for estimating the initial status of soil saturation provides a well-reproduced baseflow trend during the 30-hour period prior to storm flow concentration.

The catchment storm flow hydrographs corresponding to test cases (b) and (c) are shown in Figures 5b and 5c, respectively. The small surface flow component reproduced in test case (a) completely vanishes as field heterogeneity is smoothed. In addition, the effect of the near-surface heterogeneity on the simulated catchment storm flow response appears to be slight. This leads to the conclusion that the subsurface storm flow component is relatively insensitive to near-surface soil heterogeneity. The hydrographs of Figure 5d are obtained by varying the outlet cell value of K_s (from 3.06×10^{-5} to 3.06×10^{-8} m s^{-1}) in the functional parameter model of Equation (10) as shown in Figure 4, so as to reproduce the observed hydrograph peaks with rapid concentration of rainfall excess runoff [test case (d)]. The need for this adjustment may be posteriorly explained by the fact that the logistical difficulties in transporting water across the Bracciasco catchment may have led to premature ending of the infiltration experiments and thus the estimated hydraulic conductivities may have been overestimated owing to residual capillary forces of soils that were not completely saturated. This suspected overestimation is expected to be stronger in lowland areas, where fine-grained soils produce relatively more important capillary effects. The implemented reduction of near-surface soil conductivity with respect to observed values leads to better simulation results in terms of hydrograph peaks and recession limbs, owing to a more suitable partitioning of ground-level precipitation at the land surface over hillslope areas. However, the reproduction of the surface flow component in the initial phase of storm flow concentration is satisfactory in terms of delivered volumes but indicates an underestimation of diffusional effects in flow propagation. It is possible that this underestimation is a result of inadequately describing the rainfall excess spatial distribution in test case (d) and/or neglecting the hydraulic effect of Palù Lake on surface flow dynamics.

SUMMARY AND CONCLUSIONS

The incorporation of measured near-surface soil hydraulic conductivities, K_s, obtained from extensive field inspections in the Bracciasco catchment (Central Italian Alps) into a distributed, DEM-based hydrological modeled to satisfactory reproductions of the catchment storm flow response. In particular, the estimation procedure for initial conditions of soil saturation based on the initial outlet baseflow led to well-reproduced outlet flows prior to storm flow concentration. Numerical experiments were carried out to evaluate the effect of the observed soil heterogeneity on catchment response, considering four different test cases: (a) observed distribution of K_s; (b) uniform distribution, with average measured value of K_s; (c) functional parameter distribution of Equation (10) interpreting the observed data; and (d) functional parameter distribution of Equation (10) adjusted to calibrate surface and subsurface catchment storm flow partitioning. The results obtained showed that: (1) as far as subsurface flow is the dominant mechanism of channel flow generation, the simulated storm flow response of the Bracciasco catchment is substantially insensitive to near-surface soil heterogeneity; (2) an adjustment of the observed K_s distribution is suggested to reproduce the hydrograph peaks owing to rapid surface runoff concentration and to improve the description of recession limbs at the same time; and (3) this adjustment leads to improvement in the overall land surface partitioning of intense rainfall peaks and thus in the reproduction of surface and subsurface discharged volumes, but it may reveal the inability of the functional parameter model of Equation (10) to provide adequate descriptions of rainfall excess spatial distribution, leading to inaccurate time distribution of the surface storm flow component at the catchment outlet.

The analysis carried out in the present paper must be qualified by the facts that: (1) the combination of infiltration excess and subsurface flow mechanisms of channel flow generation allows return flow (from soil to land surface) only at the hillslope bases, neglecting the possibility of saturation excess runoff and return flow over hillslope areas; (2) rainfall was assumed to be uniformly distributed across the catchment and this may

lessen the effects the near-surface soil heterogeneity on catchment dynamics; and (3) the conductivity, K_h, of the subsuperficial drainage network and the lower soil control volume depth, Z_{low}, were determined as fitting parameters and no detailed field measurements for them were available. Although more extensive field data must be collected in order to fit and verify relationships such as Equation (10) and in order to conduct a comprehensive model validation and parameter optimization (especially for K_h and Z_{low}), the analysis carried out in the present work leads to the conclusion that water yield from upland Alpine areas (where near-surface soils are highly permeable and the water table may be several metres deep) is determined predominantly by the non-linear storage–release behaviour of complex soil and fractured rock formations as far as the storm intensity lies below the infiltration capacity of soil. Near-surface soil heterogeneity may play an important role when rainfall peaks are partitioned at the land surface, and this must be adequately described to reproduce both hydrograph peaks owing to rapid infiltration excess runoff concentration and infiltration soil inflows. The combined use of distributed non-linear soil water balances and diffusion wave subsurface flow routing provides a robust and efficient tool for describing subsurface delivery from hillslopes and this may be relevant in the distributed, DEM-based modelling of near-surface soil processes such as channel flow generation, debris flow and soil slips in Alpine areas.

REFERENCES

Bacchi, B., Bianchi, A., Bresadola, P., Massiotta, P., Pirola, A., and Sfondrini, G. 1983. 'Il bacino del Torrente Bracciasco, Valmalenco: cartografia', *Pubblicazione per il Progetto CNR 'Conservazione del Suolo: Dinamica Fluviale' no. 174*. Dipartimento di Scienze della Terra, Università degli Studi di Milano, Milano.

Bathurst, J. C. 1993. 'Flow resistance through the channel network', in Beven, K. and Kirkby, M. J. (eds), *Channel Network Hydrology*. John Wiley, New York. pp. 69–98.

Beven, K. and Germann, P. 1982. 'Macropores and water flow in soils', *Wat. Resour. Res.*, **18**, 1311–1325.

Beven, K. and Kirkby, M. J. 1979. 'A physically based, variable contributing area model of basin hydrology', *Hydrol. Sci. Bull.*, **24**, 43–69.

Boussinesq, J. 1904. 'Recherches théoriques sur l'écoulement des nappes d'eau infiltrées dans le sol et sur le débit des sources', *J. Math. Pures Appl.*, **10**, 5–78.

Brooks, B. H. and Corey, A. T. 1964. 'Hydraulic properties of porous media', *Hydrol. Pap. 3*, Colo. State Univ., Fort Collins.

Chiari, A. 1984. 'Idrologia ed idrogeologia dei bacini del Torrente Bracciasco e del Lago Palù, Valmalenco, Sondrio', *Tesi di laurea*, Dipartimento di Scienze della Terra, Università degli Studi di Milano, Milano.

Cunge, J. A. 1969. 'On the subject of a flood propagation computation method (Muskingum method)', *J. Hydraul. Res.*, **7**, 205–230.

Emmett, W. W. 1978. 'Overland flow', in Kirkby, M. J. (ed.), *Hillslope Hydrology*. John Wiley and Sons, New York. pp. 145–176.

Loague, K. 1990. 'R-5 revisited, 2. Reevaluation of a quasi-physically based rainfall-runoff model with supplemental information', *Wat. Resour. Res.*, **26**, 973–987.

Loague, K. and Gander, G. A. 1990. 'R-5 revisited, 1. Spatial variability of infiltration on a small rangeland catchment', *Wat. Resour. Res.*, **26**, 957–971.

Montgomery, D. R. and Foufoula-Georgiou, E. 1993. Channel network source representation using digital elevation models', *Wat. Resour. Res.*, **29**, 3925–3934.

Moore, I. D. and Grayson, R. B. 1991. 'Terrain-based catchment partitioning and runoff prediction using vector elevation data', *Wat. Resour. Res.*, **27**, 1177–1191.

Mosley, M. P. 1979. 'Streamflow generation in a forested watershed, New Zealand', *Wat. Resour. Res.*, **15**, 795–806.

Orlandini, S. 1998. 'A two-layer model of near-surface soil drying for time-continuous hydrologic simulations', *J. Hydrol. Emgrg., ASCE*, in press.

Orlandini, S. and Rosso, R. 1996. 'Diffusion wave modeling of distributed catchment dynamics', *J. Hydrol. Emgrg., ASCE*, **1**, 103–113.

Orlandini, S. and Rosso, R. 1998. Parameterization of stream channel geometry in the distributed modeling of catchment dynamics', *Wat. Resour. Res.*, **34**, 1971–1985.

Orlandini, S., Mancini, M., Paniconi, C. and Rosso, R. 1996. 'Local contributions to infiltration excess runoff for a conceptual catchment scale model', *Wat. Resour. Res.*, **32**, 2003–2012.

Paniconi, C. and Wood, E. F. 1993. 'A detailed model for simulation of catchment scale subsurface hydrologic processes', *Wat. Resour. Res.*, **29**, 1601–1620.

Philip, J. R. 1954. 'An infiltration equation with physical significance'. *Soil Sci.*, **77**, 153–157.

Philip, J. R. 1980. 'Field heterogeneity: some basic issues', *Wat. Resour. Res.*, **16**, 443–448.

Ponce, V. M. 1986. 'Diffusion wave modeling of catchment dynamics', *J. Hydrol. Emgrg., ASCE*, **112**, 716–727.

Ponce, V. M. and Yevjevich, V. 1978. 'Muskingum–Cunge method with variable parameters', *J. Hydr. Div., ASCE*, **104**, 1663–1667.

Richards, L. A. 1931. 'Capillary conduction of liquids through porous media', *Physics*, **1**, 318–333.

Sfondrini, G. 1986. 'Alcuni aspetti del regime idraulico di un bacino alpino: Torrente Bracciasco e Lago Palù, Valmalenco (in Italian)', in *Atti del Convegno Valmalenco Natura 1, Sondrio, 26–28 Settembre*, pp. 259–275.

Sivapalan, M., Beven, K., and Wood, E. F. 1987. 'On hydrologic similarity, 2. A scaled model of storm runoff production', *Wat. Resour. Res.*, **23**, 2266–2278.

Sloan, P. G. and Moore, I. D. 1984. 'Modelling subsurface stormflow on steeply sloping forested watersheds', *Wat. Resour. Res.*, **20**, 1815–1822.

Troch, P. A., De Troch, F. P., and Brutsaert, W. 1993a. 'Effective water table depth to describe initial conditions prior to storm rainfall in humid regions', *Wat. Resour. Res.*, **29**, 427–434.

Troch, P. A., Mancini, M., Paniconi, C., and Wood, E. F. 1993b. 'Evaluation of a distributed catchment scale water balance model', *Wat. Resour. Res.*, **29**, 1805–1817.

APPENDIX: DIFFUSION WAVE FORMULATION FOR SUBSURFACE STORM FLOWS

The superscript '(sub)' used in the section on catchment modelling to identify subsurface flow variables is omitted in the present Appendix (where all the hydraulic variables refer to subsurface flows) for simplicity of notation. The convection–diffusion Equation (6) for unconfined subsurface storm flows is derived from the continuity equation

$$\frac{\partial \Omega}{\partial t} + \frac{\partial Q}{\partial s} = q_{\mathrm{L}} \tag{A1}$$

and the simplified momentum equation

$$\frac{\partial (Y \cos \beta)}{\partial s} = S_0 - S_{\mathrm{f}} \tag{A2}$$

where s and t are the spatial and temporal coordinates, respectively, Ω is the apparent flow area, Q is the discharge, q_{L} is the lateral inflow, Y is the apparent flow depth, β is the inclination angle of the relatively impervious layer on which the flow occur, $S_0 = \sin \beta$ is the slope of this layer and S_{f} is the friction slope. Since $\partial \Omega / \partial t = \mathrm{d}\Omega / \mathrm{d}Y \cdot \partial Y / \partial t$, Equation (A1) can be written in the form

$$W \frac{\partial Y}{\partial t} + \frac{\partial Q}{\partial s} = q_{\mathrm{L}} \tag{A3}$$

$W = \mathrm{d}\Omega / \mathrm{d}Y$ being the phreatic surface width. Equations (A2) and (A3) can be combined into a single equation by taking the derivative of the first with respect to t and of the second with respect to s in order to eliminate the mixed derivative $\partial^2 Y / (\partial s \partial t)$. Incorporating the formula

$$\frac{\partial S_{\mathrm{f}}}{\partial t} = \frac{\partial S_{\mathrm{f}}}{\partial Q} \cdot \frac{\partial Q}{\partial t} + \frac{\partial S_{\mathrm{f}}}{\partial Y} \cdot \frac{\partial Y}{\partial t} \tag{A4}$$

and the expression of $\partial Y / \partial t$ given by Equation (A3) into the obtained combination equation, for $\partial q_{\mathrm{L}} / \partial s = 0$ and $\partial W / \partial s \cdot \partial Y / \partial t = 0$, yields

$$\frac{\partial^2 Q}{\partial s^2} = \frac{1}{D_{\mathrm{h}}} \left[\frac{\partial Q}{\partial t} - c_{\mathrm{k}} \left(q_{\mathrm{L}} - \frac{\partial Q}{\partial s} \right) \right] \tag{A5}$$

[which corresponds to Equation (6)], where

$$c_{\mathrm{k}} = -\frac{\partial S_{\mathrm{f}}}{\partial \Omega} \bigg/ \frac{\partial S_{\mathrm{f}}}{\partial Q} \tag{A6}$$

is the kinematic celerity and

$$D_{\mathrm{h}} = 1 \bigg/ \left(\frac{W}{\cos \beta} \frac{\partial S_{\mathrm{f}}}{\partial Q} \right) \tag{A7}$$

is the hydraulic diffusivity. Taking the derivative of the friction Equation (7) solved for S_{f}, one can obtain from Equations (A6) and (A7) the expressions of c_{k} and D_{h} given in Equations (8) and (9), respectively, where S_{f} is ultimately assumed equal to S_0 on the basis of the kinematic flow assumption.